Jour. Korean Earth Science Society, v. 28, no. 5, p. 545–555, September 2007

Validation of Ocean General Circulation Model (FMS-MOM4) in Relation with Climatological and Argo Data

You-Soon Chang[1,*], Chang-Woo Cho[1], Yong-Hoon Youn[2], and Jang-Won Seo[1]

[1]Global Environment System Research Laboratory, National Institute of Meteorological Research, Seoul 156-720, Korea

[2]Marine Meteorology Division, Korea Meteorological Administration, Seoul 156-720, Korea

Abstract: Ocean general circulation model developed by GFDL on the basis of MOM4 of FMS are examined and evaluated in order to elucidate the global ocean status. The model employs a tripolar grid system to resolve the Arctic Ocean without polar filtering. The meridional resolution gradually increases from 1/3° at the equator to 1° at 30°N(S). Other horizontal grids have the constant 1° and vertical grids with 50 levels. The ocean is also coupled to the GFDL sea ice model. It considers tidal effects along with fresh water and chlorophyll concentration. This model is integrated for a 100 year duration with 96 cpu forced by German OMIP and CORE dataset. Levitus, WOA01 climatology, serial CTD observations, WOCE and Argo data are all used for model validation. General features of the world ocean circulation are well simulated except for the western boundary and coastal region where strong advection or fresh water flux are dominant. However, we can find that information concerning chlorophyll and sea ice, newly applied to MOM4 as surface boundary condition, can be used to reduce a model bias near the equatorial and North Pacific ocean.

Keywords: Ocean general circulation model, MOM4, climatology, Argo

Introduction

The Modular Ocean Model (MOM) is designed primarily as one of the Ocean General Circulation Models (OGCMs) for the better understanding of the ocean climate system. It was mainly developed at Geophysical Fluid Dynamics Laboratory (GFDL), and has been used by many researchers worldwide.

The most recent version of MOM is version 4, which is the ocean component of Flexible Modeling System (FMS) operated in GFDL (Griffies et al., 2005). It has been estimated that the recent GFDL model are realistic and superior to the older results (Delworth et al., 2002; Gnanadesikan et al., 2006; Griffies et al., 2005; Stouffer et al., 2006; Wittenberg et al., 2006). However, a stand-alone test of the OGCM has been overlooked, despite its great significance. They all have used a fully coupled model focusing on the climate change.

*Corresponding author: you@metri.re.kr
Tel: 82-2-841-2786
Fax: 82-2-841-2787

In order to make the full use of new OGCM, MOM4, it is important to proper assess its performance. One of the basic methods to validate simulation results is the model-data comparison. The main purpose of this study is to validate MOM4 based on oceanic observation data. In this study, we compare the temperature and salinity distribution calculated from MOM4 to observational estimates over various regions. It is expected that the results presented in this study will serve as a reference for the future work with this model.

Model description

MOM employs a finite difference treatment of the primitive equations of motion using the Boussinesq and hydrostatic approximations in spherical coordinates with the Arakawa B-grid. The version used here is MOM4p0d leased on May, 2005.

The model covers the global ocean. The meridional resolution gradually increases 1/3° at the equator to 1° at 30°N(S) in order to resolve narrow features such as the equatorial undercurrent in tropics (Latif et al., 1998; Schneider et al., 2003). Other horizontal grids

have the constant 1°. The model grid is defined by the tripolar grid system of Murray (1996) for removing the spherical coordinate singularity from the Arctic Ocean, effectively. The ocean is also coupled to the GFDL sea ice model (see details at Griffies et al., 2005).

The vertical resolution is 50 depth levels where the top 22 levels are evenly spaced in the top 220 m depth. Bottom topography data used in this model is coarsened version provided by Southampton Oceanography Centre. It is a montage of that developed by Smith and Sandwell (1997) by satellite data in the region of 72S to 72N, the NOAA (1988) 5-minute global topography ETOPO5, and the International Bathymetric Chart of the Arctic Ocean.

Tracer advection is based on the third order upwind biased approach of Hundsdorfer and Trompert (1994) who employ the flux limiters of Sweby (1984). Background vertical and diapycnal mixings are parameterized by the Bryan and Lewis (1979) and KPP scheme of Large et al. (1994), which have been developed for use in global climate modeling, respectively. For the bottom boundary layer, Beckmann and Doscher's scheme is embedded (Bechmann and Doscher, 1997).

Model is mainly forced with the German Ocean Model Intercomparison Project (OMIP) (Roske, 2006) and Coordinated Ocean Reference Experiments (CORE) dataset (Large and Yeager, 2004). We specify surface boundary fluxes by data override, that is, we use one of the fluxes coming from an atmospheric model (GFDL's data portal) and replace this flux with that. For the fresh water flux, we use real fresh water flux as opposed to virtual salt fluxes. We have no restoring to surface temperature, while salinity restoring of 300 days for the first model layer is applied.

As for additional boundary conditions, we use river discharge, M2-tidal components, and chlorophyll concentration data in order to consider the effects of fresh water flux, tidal mixing, and penetrative shortwave radiation (Fig. 1).

In the real world, river properties are generally

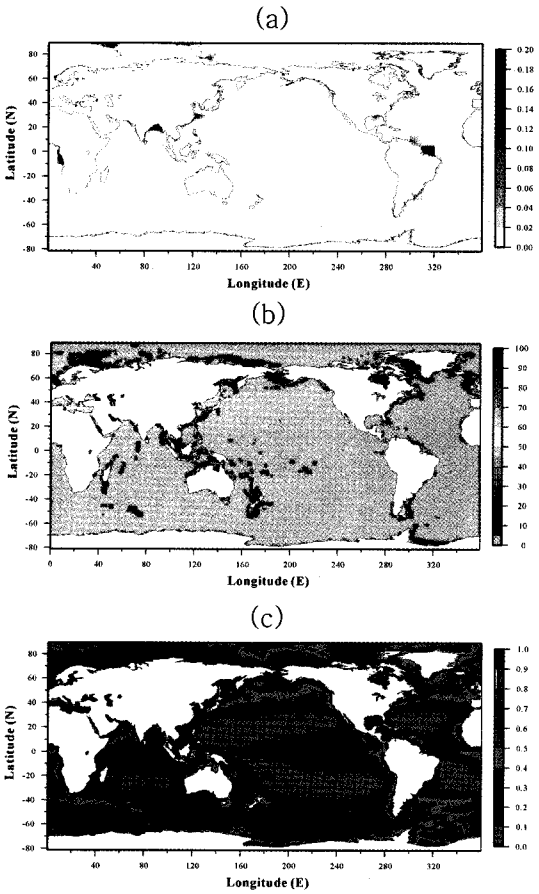

Fig. 1. Annual mean (a) river discharge (kg/m^2 · s), (b) maximum speed of the M2 tidal component (cm/s), and (c) chlorophyll concentration (mg/m^3), which are used in MOM4 as surface boundary conditions.

mixed through a vertical column due to waves and tides near the coasts (Griffies et al., 2005). So, MOM4 enhances vertical mixing of tracers in the region next to river mouths. In our study, enhanced mixing is strongest near the surface and tapers to zero at 40 m depth. We do not consider the variation of vertical diffusivity and spread over more than one river-mouth point.

Realistic and integrated tidal mixing is also important for many numerical studies (Lynch et al., 1996; Holloway, 2001; Werner et al., 2003). However, because of its small spatial scale of shallow coastal regions, this barotropic tide traditionally has been excluded from OGCM. Recently Lee et al. (2006)

summarized and investigated barotropic tidal mixing effect by using their climate model, GFDL CM2.0. MOM4 also use tidal speed as shown in Fig 1(b) to enhance the vertical shear in the computation of the Richardson number based on Lee et al. (2006).

It has been well known that variation of short penetrative radiation is largely controlled by the concentration of light-absorbing pigments associated with phytoplankton that vary over a wide range of time and space scales. Recently Nakamoto et al. (2000) addressed it in their isopycnal OGCM. Murtugudde et al. (2002) used reduced gravity OGCM coupled to an advective atmospheric mixed layer model. MOM4 allows geographical and monthly variations of the short wave penetration using climatology chlorophyll data from Sweeney et al. (2005) as shown in Fig 1(c).

Using 96 processors of GFDL High Performance Computing System (HPCS), Intel cluster of Altix computers, the model was able to complete integration for 100 years. This spin up time appears to be a sufficient for general circulation process in the ocean to have reached a quasi-equilibrium. Results described here will typically be based on monthly averages from the final year.

Results

Horizontal difference of SST and SSS with WOA01

Fig. 2 depicts the SST (Sea Surface Temperature) difference in February and August with observation-based WOA01 (World Ocean Atlas 2001) climatology. In the tropics the difference are small compared to many previous results of OGCMs which have shown chronic cold bias associated with strong equatorial upwelling (Han, 1984; Chang et al., 2005). This would be expected from the chlorophyll concentration that has been newly applied to surface boundary condition (Fig. 1(c)). High levels of chlorophyll which

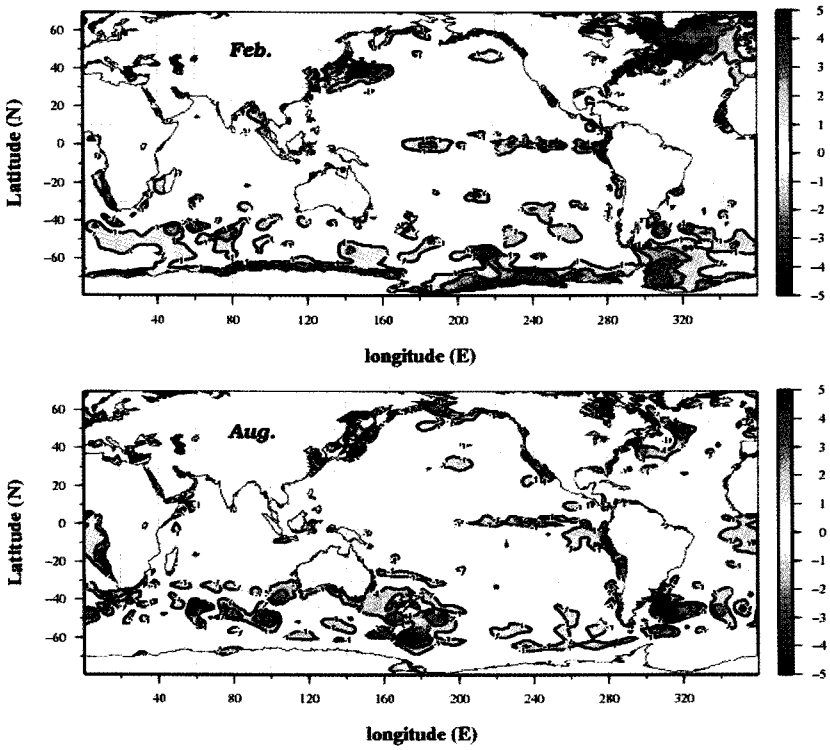

Fig. 2. Difference of sea surface temperature with WOA01 climatology in February (top) and August (bottom), respectively. Units are in °C.

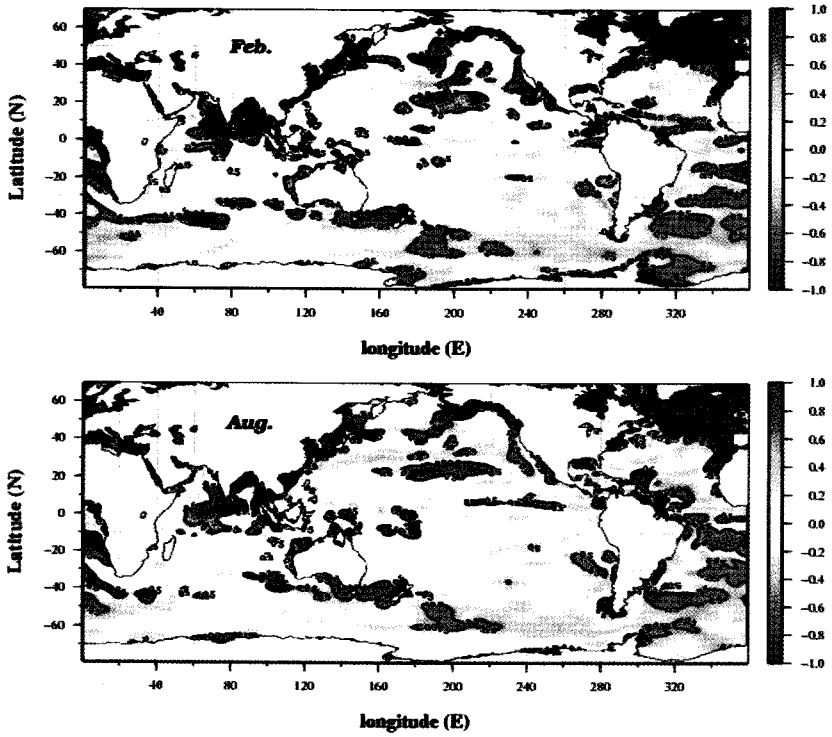

Fig. 3. The same as Fig. 2 except for sea surface salinity. Units are psu.

control the penetration of shortwave radiation along the equatorial region could reduce the cold bias, which has been suggested by Murtugudde et al. (2002). There are some larger differences, but they are restricted either to western boundary regions, coastal or high-latitudinal areas where strong advection or fresh water flux are dominant. Due to their coarse resolution, model and climatology data do not properly capture these features.

SSS (Sea Surface Salinity) difference with WOA01 is shown in Fig. 3. A positive bias exists near the northern subtropics. This problem might be associated with errors in precipitation data used to force the model. The too fresh areas match up well with the coastal regions and Northern Atlantic where river discharge, tidal mixing and sea-ice interaction are strong.

Equatorial details

Equatorial dynamics plays a crucial role in determining global climate variability, in particular through ENSO. In this section, we focus on the equatorial and western Pacific, whereas in Hawaii-Tahiti (Wyrtki and Kilonsky, 1984) and 137°E lines (Hosoda and Minato, 2003).

Left panels of Fig. 4 show a zonal geostrophic flow, temperature, and salinity distribution along the Hawaii-Tahiti transect. They show a sharper temperature gradient and tongues of high-salinity water that stretch equator-ward. These overall features are well simulated by our model (Right panels of Fig. 4). However there still remain some discrepancies between model and observed fields such as the current speed and salinity maxima. The maximum current of observed North Equatorial Countercurrent is over 40 cm/s. The eastward Equatorial undercurrent with a core speed more than 50 cm/s at 140 m depth are observed. However, model simulates their currents less than 10 cm/s (At the surface layer, model can not simulate North Equatorial Countercurrent) and more than 70 cm/s, respectively. In the subsurface around 150 m are found salinity maxima in both hemispheres,

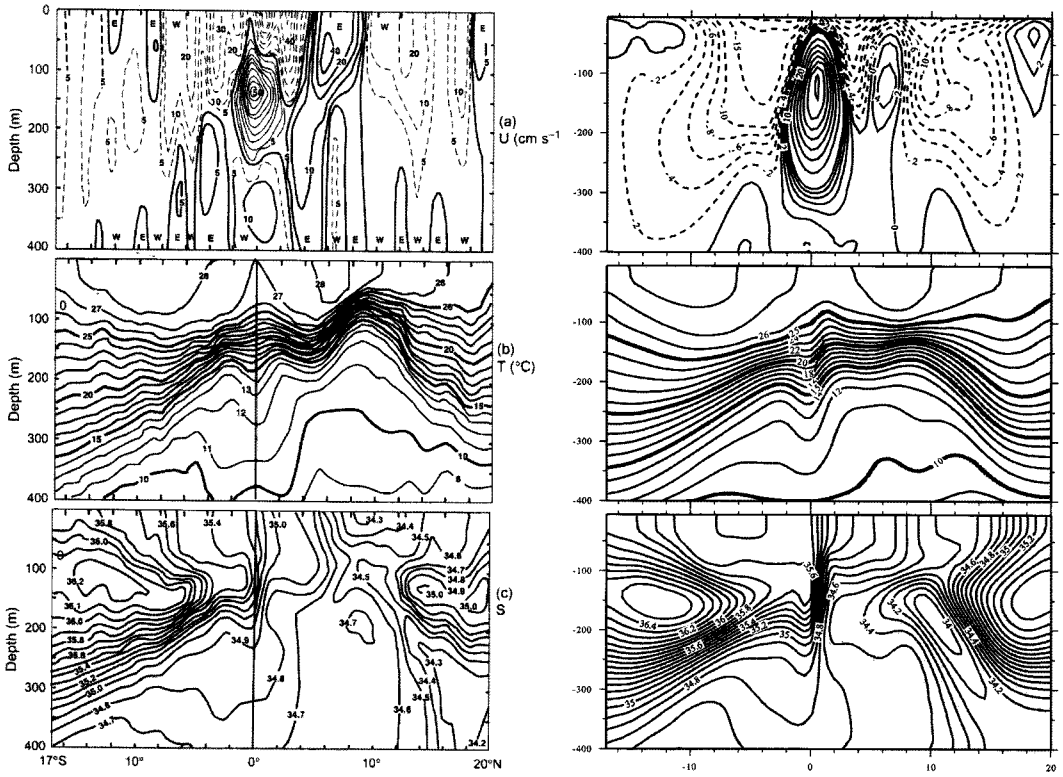

Fig. 4. Left panels show mean distributions of (a) zonal geostrophic flow (cm/s), temperature (°C), and salinity (psu) between Hawaii and Tahiti (about 150°W and 160°W), for the period April 1979-March 1980 (After Wyrtki and Kilonsky (1984)). Rights are simulated results from MOM4.

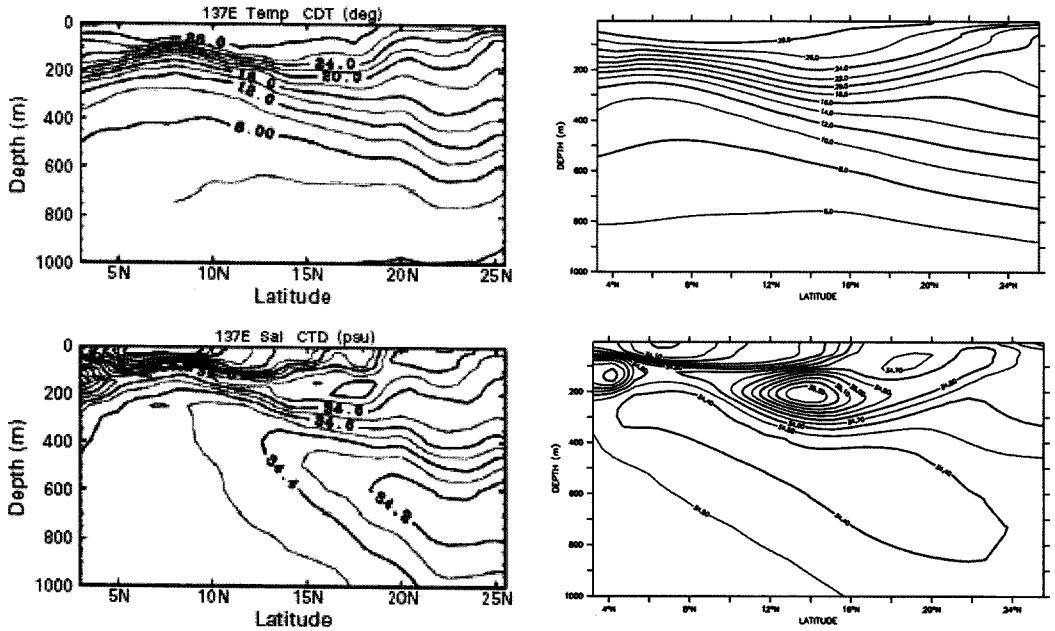

Fig. 5. Left panels show vertical sections of observed temperature and salinity along 137°E in May 2002 (After Hosoda and Minato (2003)). Rights are simulated results from MOM4.

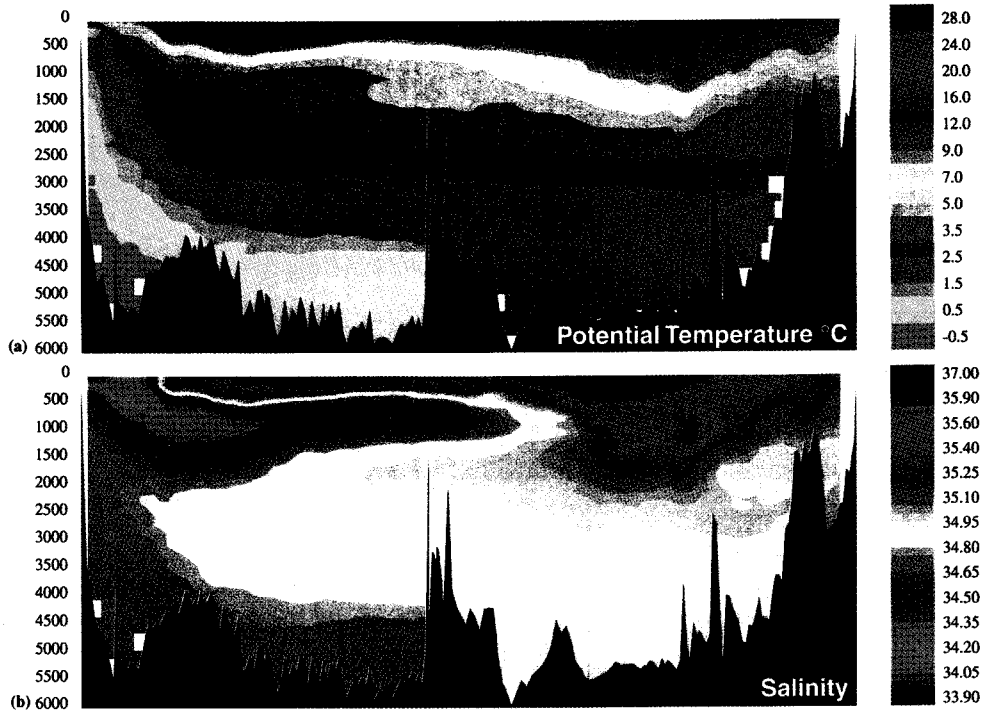

Fig. 6. Meridional WOCE section (A16) of potential temperature and salinity through the Atlantic Ocean (After Siedler et al. (2001)).

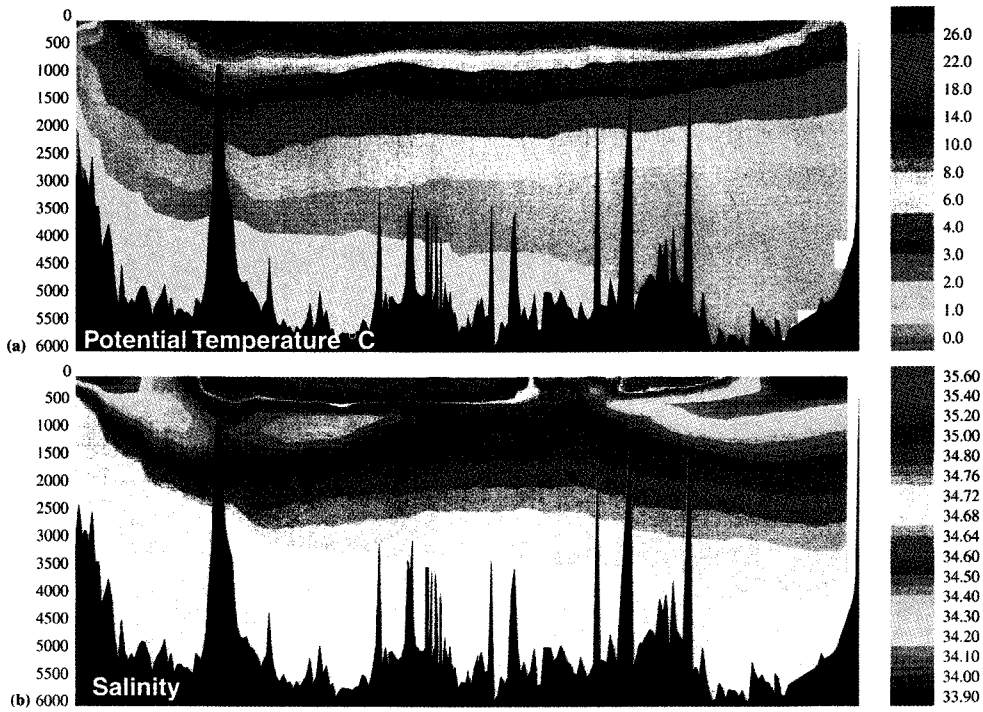

Fig. 7. The same as Fig. 6 except for P15 section.

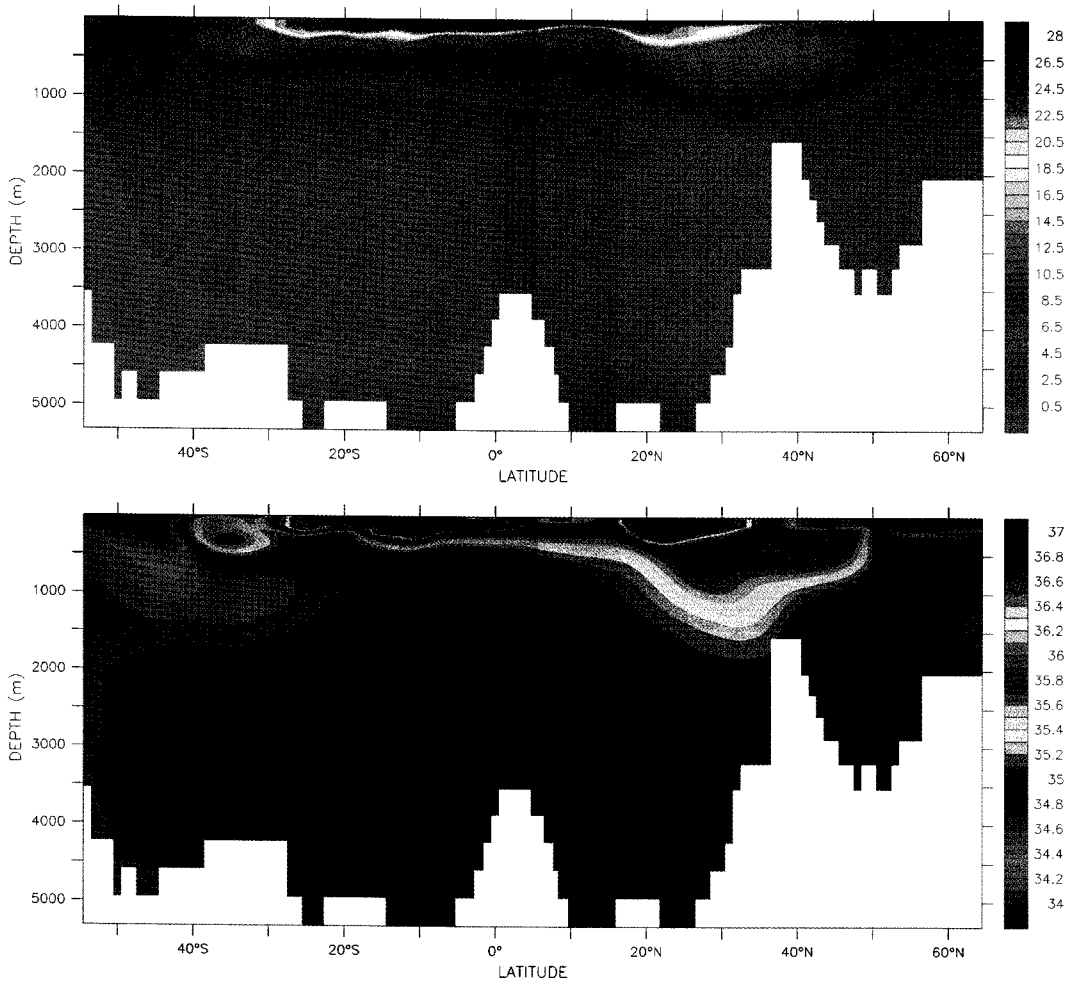

Fig. 8. Simulated results of potential temperature and salinity along the WOCE (A16) section.

whereas those of model are simulated more than 36.5 psu.

We also compare model result with observed CTD data along 137°E lines observed by Japan Meteorological Agency (Hosoda and Minato, 2003). Vertical temperature gradient from 28°C to 12°C in low latitudinal area (5 to 10°N) are larger compared to those of mid-latitudinal regions (15 to 20°N). Salinity in the mid-layer of western Pacific is also characterized by a minimum that extends equator-ward across 20°N at a core depth between 600 m and 800 m. These general features are corresponding well with the temperature and salinity section from model as shown in the right panels of Fig. 5.

Comparison with WOCE

With World Ocean Circulation Experiment (WOCE), it has been successfully explained about surface density fields, subduction process at specified ocean areas, or thermocline theory (Siedler et al., 2001). Fig. 6 (WOCE A16 line) shows the tongues of low-salinity Antarctic Intermediate water penetrating northward near the base of the subtropical gyres at depth of 800-1000m in the Atlantic Ocean. Fig. 7 (WOCE P15 line) also includes the tongue of low-salinity North Pacific Intermediate Water penetrating southward in the North Pacific at depths of about 500 m.

MOM4 coupled to GFDL sea ice model shows good performance for simulating of these subduction

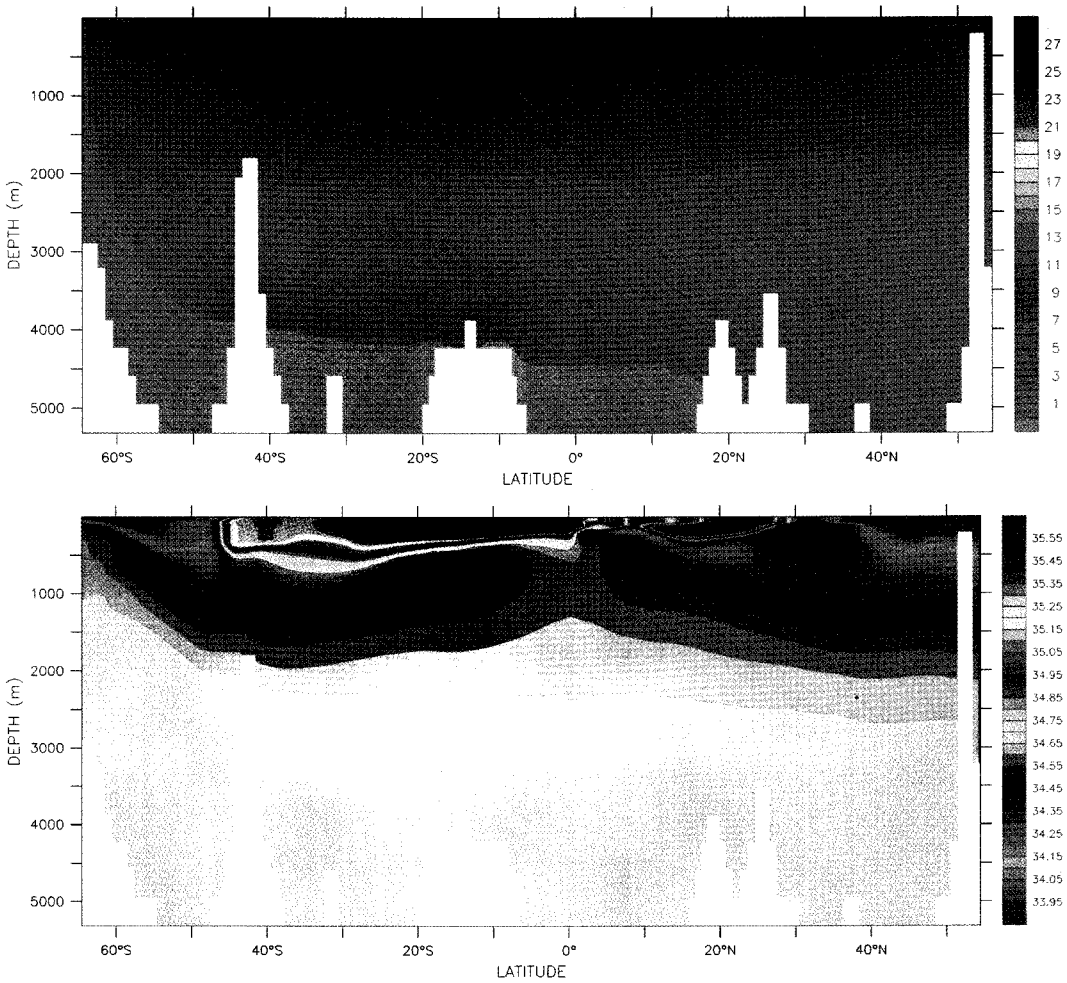

Fig. 9. The same as Fig. 8 except for P15 section.

phenomena, which is confirmed from Fig. 8 and 9. Correctly simulating these processes will be important for reliable projections of possible changes in oceanic climate changes.

Comparison with ARGO

Array for Real-time Geostrophic Oceanography (ARGO) is a new international project that is deploying more than 3000 profiling drifters in the oceans. Profiling data from Argo project have an enormous range of applications. In this section, we construct seasonal optimal estimate from Argo data in order to evaluate and validate of our model.

At first, the shipboard measurement data from 1994 to 2001 have been collected from the World Ocean Database (WOD), which were observed in the North Pacific. They were utilized for evaluate the Argo data since it has been know that salinity measurements from Argo may experience sensor drifts owing to biofouling and a variety of other problems (Wong et al., 2003; Youn et al., 2005). Therefore we calibrated the salinity drift from accurate CTD data set after basic quality checks such as time, location and pressure inversion problem. In case of salinity at the parking depth is out of 2 times standard deviation from the optimal estimate in each 5 grid, it is evaluated that the salinity profiles have abnormal drift. The drift is calibrated using the optimal estimate in the grid (METRI, 2003). After optimal estimation, about 70% of all data from Argo floats in the North

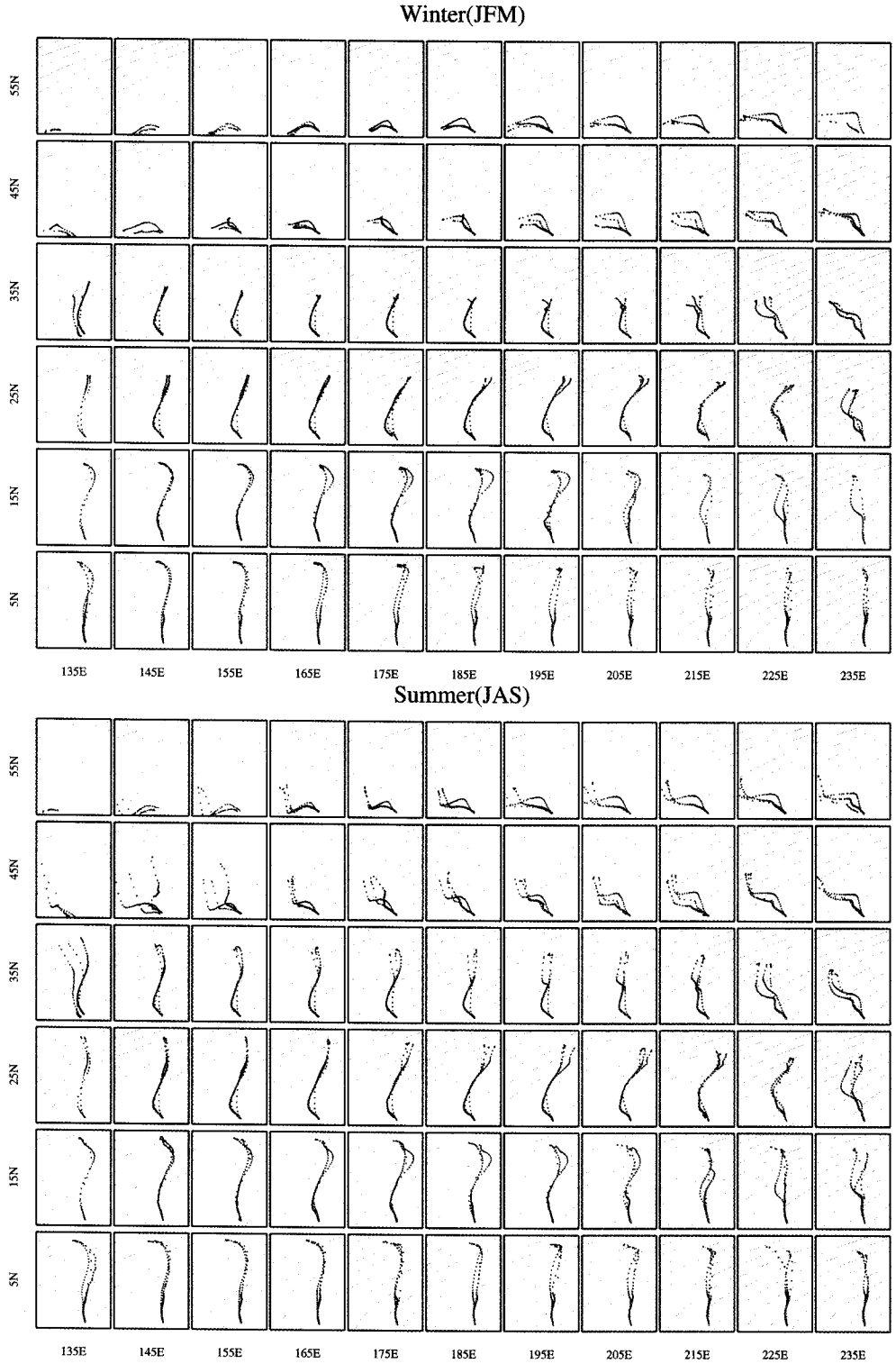

Fig. 10. Temperature-Salinity diagram in $10^{\circ}\times10^{\circ}$ grid of North Pacific Ocean in winter and summer season, respectively. Blue lines are optimal estimates based on observed Argo data, green lines are climatological Levitus data, and red lines are simulated results from MOM4.

Pacific are remained, which used for our model validation.

Fig. 10 shows the temperature-salinity relationship every 10 grid of the North Pacific in winter and summer season, respectively. For the simple comparison, Argo (blue dots), Levitus (green dots), and MOM4 (red dots) data are all spatio-temporally averaged within every 10 degree and 3 months. We estimate that MOM4 resolved well overall variation of water mass in the North Pacific. Specifically around the high-latitudinal region in winter season, it could be improved to simulate the characteristics of salinity variation at the low temperature condition. This result may come from additional boundary conditions such as fresh water and sea-ice effect, which have not been considered in previous version of MOM (METRI, 2003). However, there are some discrepancies around western boundary region in summer season. We can find overshooting of Kuroshio Current is still remains as one of the systematic problems in OGCMs.

Summary and Conclusion

In this study, we compared the temperature and salinity distribution simulated from MOM4 to observational estimates over various regions in order to make full use of new OGCM, which is recently released by GFDL. MOM4 was coupled to the GFDL sea ice model and considered effects of the tide, fresh water and chlorophyll concentration as well. As for reference for validation of model, we used Levitus, WOA01 climatology, serial CTD observations, WOCE and Argo data.

We concluded that general features of the world ocean circulation are well simulated compared to other previous OGCM versions except for western boundary and coastal region where strong advection or fresh water flux are dominant. However, we found that tide and fresh water that are newly used as surface boundary conditions could reduce model bias near the equatorial and North Pacific Ocean. Sensitivity analysis will be required to estimate the effects of additional boundary conditions in our further studies.

It is expected that the results presented in our study will serve as a reference for future work with this model.

Acknowledgment

Authors would like to thank prof. Y. Noh and anonymous reviewer for their valuable comments. This study was carried out under the project, "Study on the Monitoring of the Global Ocean Variability with ARGO program" at the Meteorological Research Institute/KMA.

References

Beckmann, A. and Doscher, R., 1997, A method for improved representation of dense water spreading over topography in geopotential coordinate models, Journal of Physical Oceanography, 27, 581-591.

Bryan, K. and Lewis, L.J., 1979, A water mass model of the world ocean, Journal of Geophysical Research, 84, 2503-2517.

Chang, Y.-S., Cho, C.-W., and Youn, Y.-H., 2005, Redistribution of subsurface water mass in the Pacific Ocean simulated by an ocean general circulation model. Journal of the Korean Meteorological Society, 41 (6), 1089-1100.

Delworth, T.L., Stouffer, R., Dixon, K., Spelman, M., Knutson, T., Broccoli, A., Kushner, P., and Wetherald, R., 2002, Review of simulations of climate variability and change with the GFDL R30 coupled climate model. Climate Dynamics, 19, 555-574.

Gnanadesikan, A., Dixon, K.W., Griffies, S.M., Balaji, V., Barreiro, M., Beesley, J.A., Cooke, W.F., Delworth, T.L., Gerdes, R., Harrison, M.J., Held, I.L., Hurlin, W.J., Lee, H.-C., Liang, Z., Nong, G., Pacanowski, R.C, Rosati, A., Russell, J., Samuels, B.L., Song, Q., Spelman, M.J., Stouffer, R.J., Sweeney, C.O., Vecchi, G., Winton, M., Wittenberg, A.T., Zeng, F., Zhang, R., and Dunne, J.P., 2006, GFDL's CM2 global coupled climate models. Part II: The baseline ocean simulation. Journal of Climate, 19 (5), 675-697.

Griffies, S.M., Gnanadesikan, A., Dixon, K.W., Dunne, P., Gerdes, R., Harrison, M.J., Rosati, A., Russell J.L., Samuels, B.L., Spelman, M.J., Winton, M., and Zhang, R., 2005, Formulation of an ocean model for global climate simulations. Ocean Science, 1, 45-79.

Han, Y.-J., 1984, A numerical world ocean general circulation model. Part II. A baroclinic experiment. Dynamics of Atmosphere and Oceans, 8, 444-480.

Holloway, P., 2001, A regional model of the semidiurnal internal tide on the Australian North West shelf. Journal of Geophysical Research, 106, 19625-19638.

Hosoda, S. and Minato, S., 2003, Objective analysis with Argo float and TRITON buoy data for temperature and salinity fields in the Pacific Ocean. Report of Japan Marine Science and Technology Center, 48, 67-83.

Hundsdorfer, W. and Trompert, R., 1994, Method of lines and direct discretization: A comparison for linear advection. Applied Numerical Mathematics, 469-490.

Large, W.G., McWilliams, J.C., and Doney, S.C., 1994, Oceanic vertical mixing: A review and a model with a nonlocal boundary layer parameterization. Reviews of Geophysics, 32, 363-403.

Large, W. and Yeager, S., 2004, Diurnal to decadal global forcing for ocean and sea-ice models: The data set and flux climatologies. NCAR. Technical Note: NCAR/TN-460+STR. CGD Division of the National Center for Atmospheric Research.

Latif, M., Anderson, D., Barnett, T., Cane M., Kleeman, R., Leetmaa, A., O'Brien, J., Rosati, A., and Schneider, E., 1998, A review of the predictability and prediction of ENSO. Journal of Geophysical Research, 103, 14375-14393.

Lee, H.-C., Rosati, A., and Spelman, M., 2006, Barotropic tidal mixing effects in a coupled climate model: Oceanic conditions in the Northern Atlantic. Ocean modeling, 11, 464-477.

Lynch, D.R., Ip, J.T.C., Naimie, C.E., and Wener, F.E., 1996, Comperhensiver coastal circulation model with application to the Gulf of Maine. Continental shelf Research, 16, 875-906.

Meteorological Research Institute (METRI), 2003, A study on the monitoring of the global ocean variability with ARGO program (II). MR030M10, 322 p.

Murray, R.J., 1996, Explicit generation of orthogonal grids for ocean models. Journal of Computational Physics, 126, 251-273.

Murtugudde, R., Beauchamp, J., McClain, C.R., Lewis, M., and Busalacchi, A.J., 2002, Effects of penetrative radiation on the upper tropical ocean circulation. Journal of Climate, 15, 470-486.

Nakamoto, S., Prasanna Kumar, S., Oberhuber, J., Muneyama, K., and Frouin, R., 2000, Chlorophyll modulation of sea surface temperature in the Arabian Sea in a mixed-layer isopycnal general circulation model. Geophysical Research Letter, 27, 747-750.

NOAA, 1988, Data announcement 88-MGG-02, Digital relief of the surface of the earth. NOAA, National Geophysical Data Center Boulder, Colorado.

Roske, F., 2006, A global heat and freshwater forcing dataset for ocean models. Ocean Modelling, 11, 235-297.

Schneider, E., DeWitt, D., Rosati, A., Kirtman, B., Link, J., and Tribbia, J., 2003, Retrospective ENSO forecasts: sensitivity to atmospheric model and ocean resolution. Monthly Weather Review, 131, 3038-3060.

Siedler G., Church. J., and Gould J., 2001, Ocean circulation and climate: Observing and modeling the global ocean. Academic press, San Diego, CA, USA, 715 p.

Smith, W.H.F. and Sandwell, D.T., 1997, Global seafloor topography from satellite altimetry and ship depth soundings. Science, 277, 1957-1962.

Stouffer, R.J., Broccoli, A.J., Delworth, T.L., Dixon, K.W., Gudgel, R., HELD, I., Hemler, R., Knutson, T., LEE, H.-C., Schwarzkopf, M.D., Soden, B., Spelman, M.J., Winton, M., and Zeng, F., 2006, GFDL's CM2 global coupled climate models. Part IV: Idealized climate response. Journal of Climate, 19 (5), 723-740.

Sweby, P., 1984, High-resolution schemes using flux limiters for hyperbolic conservation-laws. SIAM Journal of Numerical Analysis, 21, 995-1011.

Sweeney, C., Gnanadesikan, A., Griffies, S.M., Harrison, M., Rosati, A., and Samuels, B., 2005, Impacts of shortwvae penetration depth on large-scale ocean circulation and heat transport. Journal of Physical Oceanography, 35, 1103-1119.

Werner, S.R., Beardsley, R.C., Lentz, S.T., Hebert, D.L., and Oakey, N.S., 2003, Observations and modeling of the tidal bottom boundary layer on the southern flank of Georges Bank. Journal of Geophysical Research, 108 (C11), 8005. doi:10.1029/2001JC001271.

Wittenberg, A., Rosati, A., Lau, G., and Ploshay, J., 2006, GFDL's CM2 global coupled climate models. Part III: Tropical pacific climate and ENSO. Journal of Climate, 19 (5), 698-722.

Wong, A.P.S., Johnson, G.C., and Owens, W.B., 2003, Delayed-mode calibration of autonomous CTD profiling float salinity data by θ-S climatology. Journal of Atmosphere and Oceanic Technology, 20, 308-318.

Wyrtki, K., and Kilonsky, B., 1984, Mean water and current structure during the Hawaii-to-Tahiti shuttle experiment. Journal of Physical Oceanography, 14, 242-254.

Youn, Y.-H., Lee, H., Chang, Y.-S., and Thadathil, P., 2005, Validation of salinity data from ARGO floats: Comparison between the older ARGO floats and that of later deployments. Journal of the Korean Earth Science Society, 26 (2), 115-129.

Manuscript received: 7 August 2006
Revised manuscript received: 29 December 2006
Manuscript accepted: 15 January 2007